Chapter 2

Mineralogy and Geochemistry of Sub-Bituminous Coal and Its Combustion Products from Mpumalanga Province, South Africa

S. A. Akinyemi, W. M. Gitari, A. Akinlua and L. F. Petrik

Additional information is available at the end of the chapter

http://dx.doi.org/10.5772/50692

1. Introduction

Coal forms from the accumulation and physical and chemical alteration of plants remains that settle in swampy areas and form peat, which thickens until heat and pressure transform it into the coal we use. The coal we use is combustible sedimentary rock composed of carbon, hydrogen, oxygen, nitrogen, sulphur, and various trace elements (it has a carbonaceous content of more than 50 % by weight and more than 70 % by volume). As much as 70 % of the South African estimated coal reserve is located in the Waterberg, Witbank, and Highveld coalfields, as well as lesser amounts in the Ermelo, Free State and Springbok Flats coalfields. However, the Witbank and Highveld coalfields are approaching exhaustion (estimated 9 billion tons of recoverable coal remaining in each), while the coal quality or mining conditions in the Waterberg, Free State and Springbok Flats coalfields are significant barriers to immediate, conventional exploitation [1]. South Africa is the third largest coal producer in the world, and coal accounts for 64 % of South Africa's primary energy supply [2]. Electricity generation accounts for 61 % of the total coal consumption in South Africa and more than 90 % of the country's electricity requirements are provided for by coal-fired power plants [2]. South African coals are generally low in sulphur, nitrogen and phosphorus, and in the case of the first two the contents are dependent on maceral composition and rank [3, 4].

The inorganic elements in coal can have profound environmental, economic, technological and human health impacts [5, 6]. Consequently, knowledge of their concentration is necessary when evaluating coals for combustion and conversion and also to evaluate potential negative environmental and health impacts resulting from coal use. Trace elements

in coal are emitted into flue gas, fly ash or bottom ash of combustion plants. In a flue gas stream, trace elements are fixed in ash particles and in by-products such as gypsum and sludge if wet flue gas desulphurization unit is equipped.

Coal fly ash is a solid residue from the combustion processes of pulverised coal for the production of electrical power in power generating stations, especially when low-grade coal is burnt to generate electricity [7, 8, 9]. The coal burning power stations in the Mpumalanga Province, South Africa generates over 36.7 Mt of fly ash annually in which only 5 % is currently utilized, the rest being disposed of in the ash dams, landfills, or ponds [9, 10]. During combustion, mineral impurities in the coal, such as clay, feldspars, and quartz, are fused in suspension and float out of the combustion chamber with exhaust gases. As the fused material rises, it cools and solidifies into spherical glassy particles called fly ash [11]. The properties of the coal fly ash depend on the physical and chemical properties of the parent coal, coal particle size, the burning process and the type of ash collector.

This article presents results obtained from mineralogical and chemical characterization of coal and its combustion products from a coal burning power station in the Mpumalanga Province, South Africa. The main objective of the study is to understand the role of combustion process, chemical interaction of fly ash with ingressed CO_2 and percolating rain water on the mineralogy and chemical compositions of fly ash.

2. Methodology/research approach

2.1. XRF and LA-ICPMS analyses

Pulverised coal samples and its combustion products were analysed for major element using Axios instrument (PANalytical) with a 2.4 kWatt Rh X-ray Tube. Further, the same set of samples were analysed for trace element using LA-ICPMS instrumental analysis. LA-ICP-MS is a powerful and sensitive analytical technique for multi-elemental analysis. The laser was used to vaporize the surface of the solid sample and it was the vapour, and any particles, which was then transported by the carrier gas flow to the ICP-MS. The detailed procedures for sample preparation for both analytical techniques are reported below.

2.1.1. Fusion bead method for Major element analysis

- Weigh 1.0000 g ± 0.0009 g of milled sample
- Place in oven at 110 ºC for 1 hour to determine H_2O^-
- Place in oven at 1000 ºC for 1 hour to determine LOI
- Add 10.0000 g ± 0.0009 g Claisse flux and fuse in M4 Claisse fluxer for 23 minutes.
- 0.2 g of $NaCO_3$ was added to the mix and the sample+flux+$NaCO_3$ was pre-oxidized at 700 °C before fusion.
- Flux type: Ultrapure Fused Anhydrous Li-Tetraborate-Li-Metaborate flux (66.67 % $Li_2B_4O_7$ + 32.83 % $LiBO_2$) and a releasing agent Li-Iodide (0.5 % LiI).

2.1.2. Pressed pellet method for Trace element analysis

- Weigh 8 g ± 0.05 g of milled powder
- Mix thoroughly with 3 drops of Mowiol wax binder
- Press pellet with pill press to 15 ton pressure
- Dry in oven at 100 ºC for half an hour before analysing.

2.2. Loss on ignition determination

Loss on Ignition (LOI) is a test used in XRF major element analysis which consists of strongly heating a sample of the material at a specified temperature, allowing volatile substances to escape or oxygen is added, until its mass ceases to change. The L.O.I. is made of contributions from the volatile compounds H_2O^+, OH^-, CO_2, F^-, Cl^-, S; in parts also K^+ and Na^+ (if heated for too long); or alternatively added compounds O_2 (oxidation, e.g. FeO to Fe_2O_3), later CO_2 (CaO to $CaCO_3$). In pyro-processing and the mineral industries such as lime, calcined bauxite, refractories or cement manufacture, the loss on ignition of the raw material is roughly equivalent to the loss in mass that it will undergo in a kiln, furnace or smelter.

2.3. XRD analysis

Coal samples and its combustion products were analysed for mineralogical composition by X-ray diffraction (XRD). A Philips PANalytical instrument with a pw 3830 X-ray generator operated at 40 kV and 25 mA was used. The pulverised samples were oven-dried at 100 °C for 12 h to remove the adsorbed water. The samples were pressed into rectangular aluminium sample holders using an alcohol wiped spatula and then clipped into the instrument sample holder. The samples were step-scanned from 5 to 85 degrees 2 theta scale at intervals of 0.02 and counted for 0.5 sec per step.

2.4. Scanning Electron Microscopy and Electron Dispersive X-ray Spectroscopy (SEM/EDS)

Microstructural and chemical composition investigations of coal and coal ash were carried out by scanning electron microscopy/electron dispersive x-ray spectroscopy (SEM/EDS). For SEM/EDS aluminium stubs were coated with carbon glue; when the glue was dry, but still sticky; a small amount of powder residue samples was sprinkled onto the stub. The excess residue sample powder was tapped off and the glue allowed complete drying. The residue samples were then coated with carbon in an evaporation coater and were ready for analysis with the SEM. The SEM is an FEI Nova NanoSEM (Model: Nova NanoSEM 230); The EDS analyses were determined at 20 Kv and 5 mm working distance. The EDS detector is an Oxford X-Max (large area silicon drift detector) using the software program INCA-(INCAmicaF+ electronics and INCA Feature particle analysis software).

2.5. Transmission Electron Microscopy (TEM)

Pulverized sample (~1-2) g of the coal and coal ash samples was poured into a small conical container while little amount of ethanol was added to the sample to serve as medium for solution. This solution was then placed inside the centrifuge for few minutes (5 mins), drops of the stirred solution was then placed on a labelled 200 μm and 400 μm of copper grid underlain by a filter paper with a hot lamp light focused directly on the samples to dry up the earlier added ethanol. The resultant mixture was placed inside the air gun channel so as to project the beam on it for image analysis at a nanometric scale. The TEM analysis of study was carried out on TECHNAI G^2 F20 X-TWIN MAT 200Kv field emission transmission electron microscopy.

2.6. Proximate and ultimate analyses

Proximate and ultimate analyses were performed on coal samples based on ASTM Standards [12]. All runs were repeated to check the instrument's results repeatability and reproducibility.

3. Results and discussion

3.1. Mineralogy of coal

The XRD analytical results show that the pulverized coal used in the combustion process in the power station mainly composed of siliceous mineral such as quartz (SiO_2), kaolinite [$Al_2(SiO_2O_5)(OH)_4$)] and the non-siliceous mineral for instance potassium selenium chloride (K_2SeCl_6) and little quantities of pyrite (FeS_2) (Fig. 1). The mineral suites in the coal samples used in the present study are consistent with the previous studies [4, 13, 14, 15, 16, 17). Kaolinite is uniformly distributed in the coal samples. This mineral is commonly present in coal as two species with different crystallinity, namely a low crystallinity detrital kaolinite and a high crystallinity neomorphic kaolinite. These genetic types have been described earlier [18, 19]. Kaolinite contains water bound within their lattices.

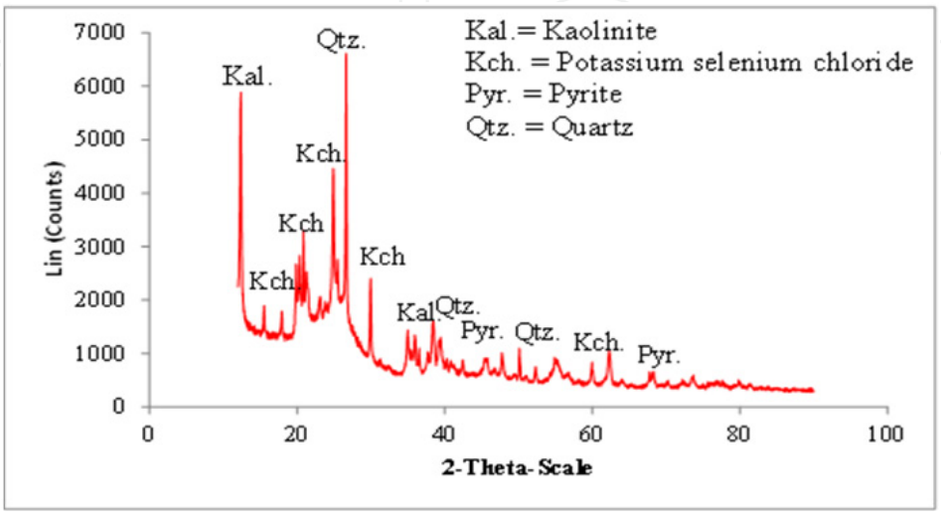

Figure 1. XRD spectra for the pulverised coal sample used in coal fired power station

All of the water is lost during the high-temperature ashing. Pyrite is the main species of sulfur oxidation in the coal samples studied. Pyrite occurs as typical syngenetic framboidal, euhedral and massive cell filling forms [20]. This mineral shows a highly inhomogeneous distribution in the coal samples. Pyrite is probably the most environmentally interesting mineral in the run of mine and beneficiation of coals and their generated wastes because of its propensity to oxidize during weathering and production of sulphuric acid.

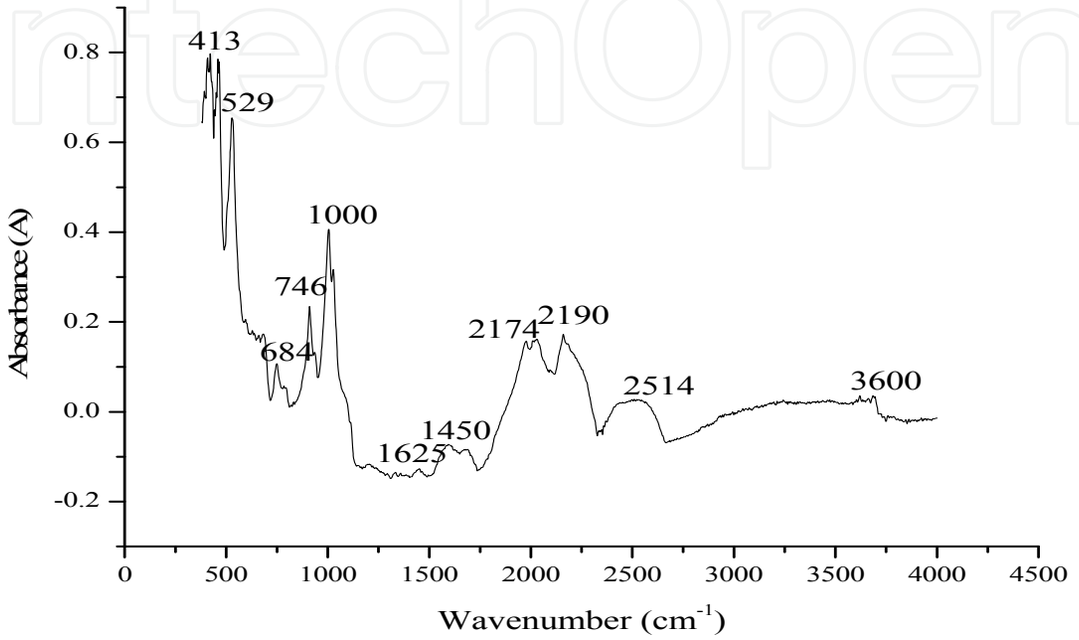

Figure 2. Infrared (FTIR) spectra of coal sample

Pyrite is transformed to hematite and sulfur dioxide during coal incineration at 815°C [20]. Some of the sulfur dioxide may remain combined with calcium in the ash, but much is lost [21]. The weathering of pyrite produces acid conditions that may leach trace elements associated with the pyrite and other constituents in the coal [22]. Quartz is the most common mineral in the coal samples studied. This mineral has mostly detrital genesis [23]. The shape of the quartz grains is rounded to semi-rounded, indicating an intensive transport before their deposition in the basin. The content of quartz is also high in the coal fly ash because this mineral is commonly stable/inert at combustion conditions (Fig. 3).

3.2. Mineralogy of weathered drilled ash cores

The mineralogical analysis by depth of the core ash samples was carried out with X- ray diffraction technique (XRD). This is to better understand the mineralogical changes (i.e. secondary phases) under the real dry disposal conditions. The experimental protocol for this section is presented in section 2.3. The results of the XRD analysis of samples of the drilled weathered dry disposed fly ash aged 2 week, 1 year and 20-year-old showed quartz (SiO_2) and mullite ($3Al_2O_3{\cdot}2SiO_2$) as main crystalline mineral phases (Fig. 3). Other minor mineral phases identified are; hematite (Fe_2O_3), calcite ($CaCO_3$), lime (CaO), anorthite ($CaAl_2Si_2O_8$), mica ($Ca(Mg,Al)_3(Al_3Si)O_{10}(OH)_2$) and enstatite ($Mg_2Si_2O_6$). This is in general agreement with

mineralogy reported for other coal fly ashes [24, 25, 26, 27, 28, 29].The eight phases observed in every sample are considered to be characteristic phase assemblages for Class F fly ash. The XRD results obtained from 2-week-old dry disposed fly ash show similar mineralogical composition to the weathered ash except for the absence of calcite and mica. Lime (CaO) presence in coal fly ash may be due to the heat transformation of dolomite mineral or decarbonation of calcite entrained in feed stock coal [30]. The mullite present in fly ash was formed by the decomposition of kaolinite [31], which is entrapped in the parent coal. The gradual reduction in pore water pH is due to chemical interaction of fly ash with ingressed CO_2 and percolating rain water. Calcite formation is attributed to chemical weathering due to over time reduction in pore water pH. Previous study had proved that calcite precipitation in weathered fly ash is as a result of chemical interactions of calcium oxide (lime) rich fly ash with ingressed CO_2 [32]..

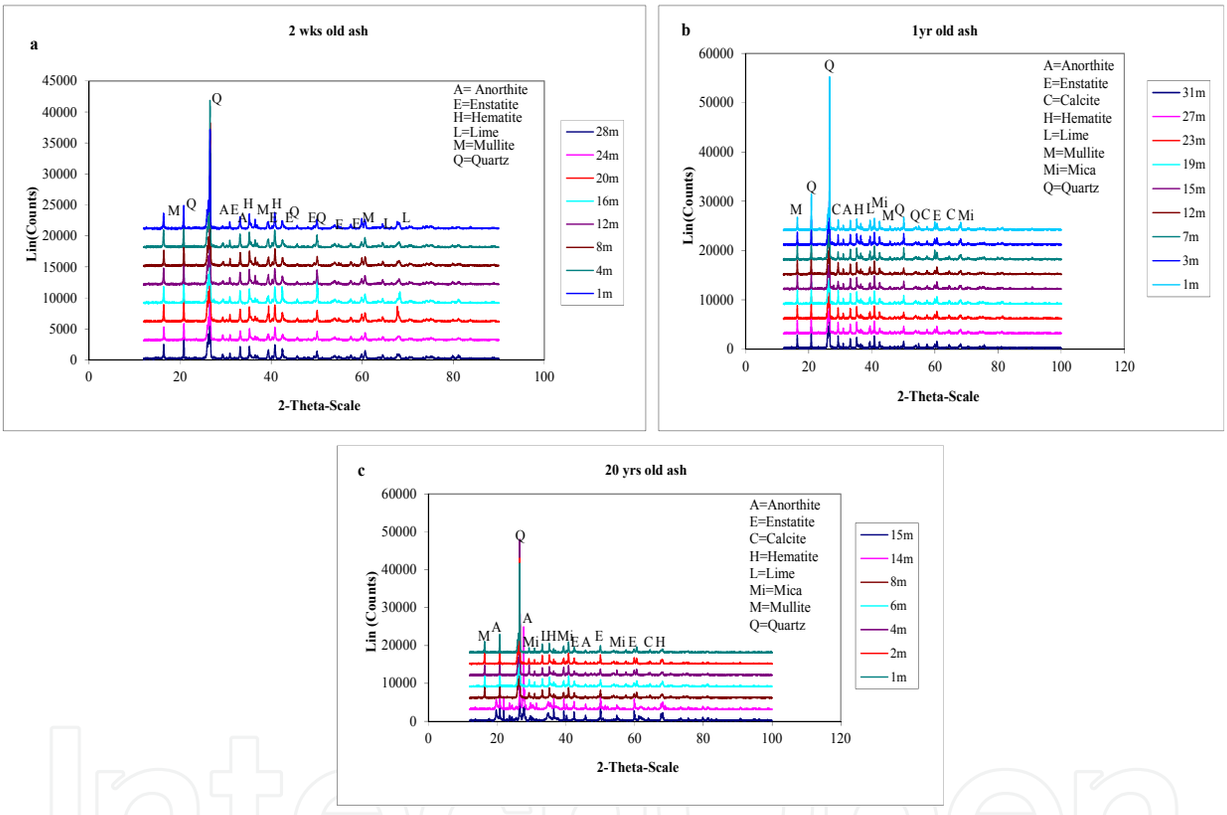

Figure 3. XRD spectra for the dry disposed ash dumps: (a) 2-week-old (T 87) not irrigated dry ash dump (b) 1-year-old (AMB 83) irrigated and quenched with high salient effluents (n = 2) (c) 20-year-old irrigated and quenched with fresh water.

Previous study has shown that the statistical variations in peak height on the same phase of ash samples could be used to assess the homogeneity and stability of different mineralogical phases [33]. A statistical consideration of the variations in the ashes peak heights for the different phases was used here to appraise the mineralogical distribution and chemical heterogeneity among the coal fly ash samples. Figures 4-6 presents the summary of the mean peak heights of mineral phases determined by XRD analysis of the 1 year, 8 year and 20-year-old ash core samples drawn from different depths of the dumps respectively. The eight phases observed in every sample are considered to be characteristic phase

assemblages for Class F fly ash. This assemblage presented in Figure 4 consisted of quartz, anorthite (residual coal minerals), mullite, calcite, hematite, mica, enstatite and lime.

In the 1-year-old ash cores, the most prominent mineral phase is quartz having a peak of almost double that of the other mineral phases in all the core samples from all depths (0-31m). The peak height of quartz mineral showed a decreasing trend with increasing depth of 1-year-old ash dump (Figure 3). This observed trend showed strong correlation with flushing/leaching of SiO_2 and Al_2O_3 in the ash dump [34]. Thus, the quartz mineral peak height is indicative of rapid dissolution/weathering of aluminosilicate mineral within 1 year of ash dumping. Other mineral phases such ash mullite; calcite, hematite, enstatite, lime, anorthite and mica showed similar trend in the 1 year and 20-year-old ash dumps (Figures 4 and 6). The prominent presence of the quartz peak in the upper depths is due to flushing of other soluble matrix in the fly ash and the mineral phase quartz is easily detectable by XRD indicating there is relative increase in concentration in the upper depth

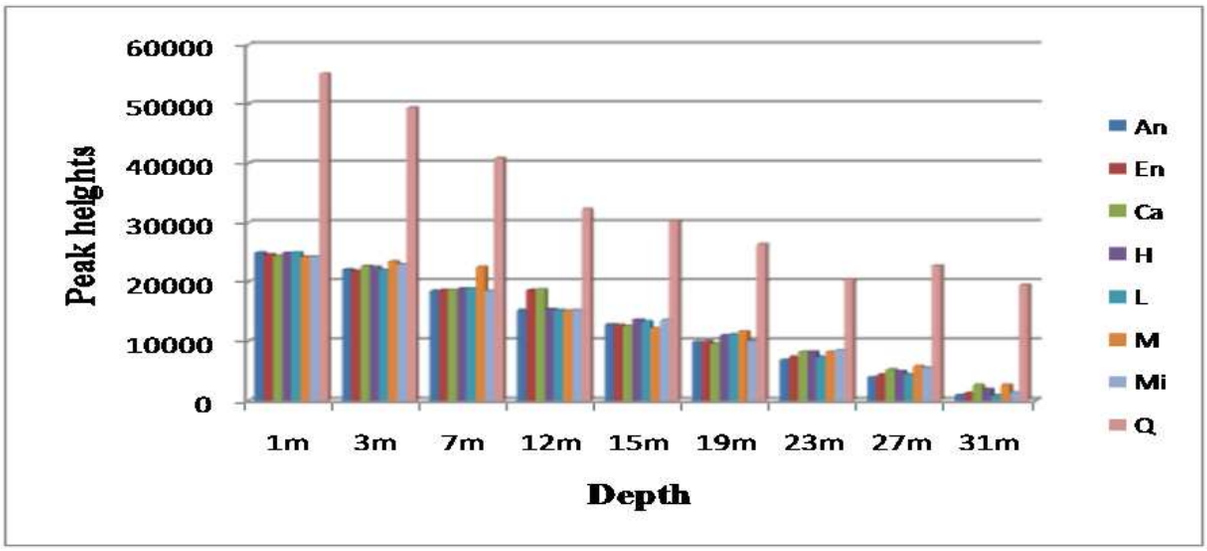

Figure 4. Bulk XRD mineral mean peak heights in 1-year-old (AMB 83) Tutuka ash cores (An=anorthite, En=enstatite, Ca=calcite, H=hematite, L=lime, M=mullite, Mi=mica, Q=quartz).

The mineral peak height in the 8-year-old section of the ash dump showed anomalous trend which may be ascribed to in-homogenous irrigation with high saline effluent (brine). This implied that the 8-year-old section has received much of high saline effluents than 1 year and 20-year-old sections of the ash dump.

The statistical result is shown in Table 1. The relative standard deviation (RSD) in the peak heights of 1-year-old drilled core (Figure 4 and Table 1) showed highly significant variations which could be classified into 2 groups:

< 40 % Quartz

57-65 % Anorthite, Enstatite, Mica, Mullite, Hematite, Calcite and Lime

The relative standard deviation (RSD) of quartz phase (being < 40 %) indicates less in-homogeneity among the coal fly ash mineral phases. There are however more variation (57-

65 %) in the peak heights of the following mineral phases, namely anorthite, enstatite, mica, mullite, calcite and lime.

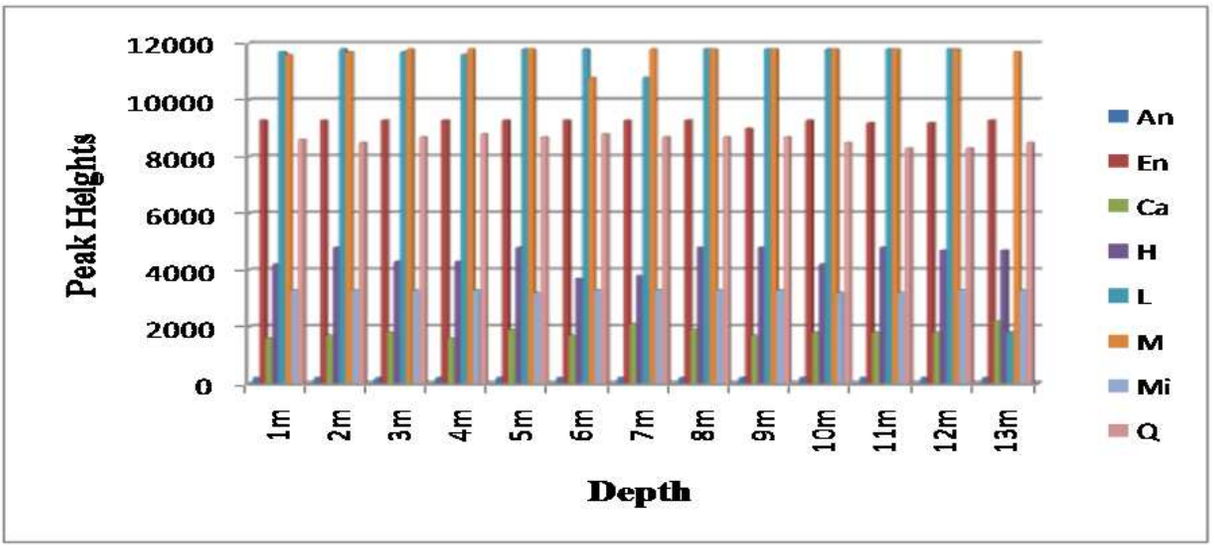

Figure 5. Bulk XRD mineral mean peak heights in 8-year-old (AMB 81) Tutuka ash cores (An=anorthite, En=enstatite, Ca=calcite, H=hematite, L=lime, M=mullite, Mi=mica, Q=quartz).

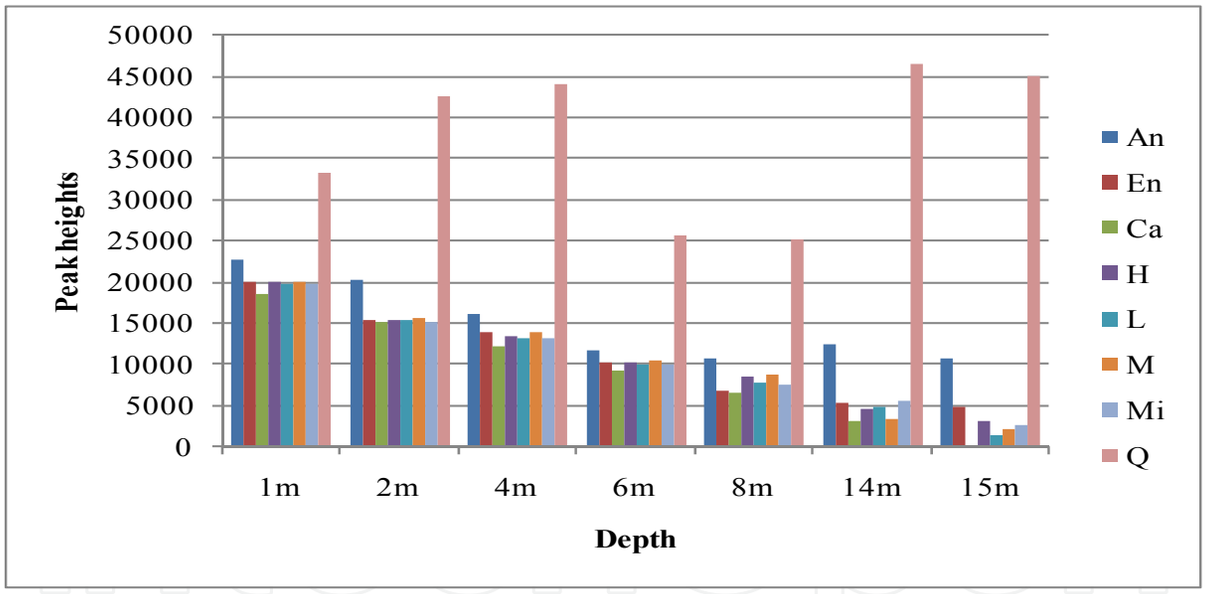

Figure 6. Bulk XRD mineral mean peak heights in 20-year-old (AMB 79) Tutuka ash cores (An=anorthite, En=enstatite, Ca=calcite, H=hematite, L=lime, M=mullite, Mi=mica, Q=quartz).

The in-homogeneous distribution of the calcite mineral phase could be attributed to continuous weathering occasioned by ingress of CO_2. There is a direct relationship between the calcite mineral phase peak heights and CaO (weight %). The depletion or enrichment of CaO (weight %) in coal fly ash agrees with the peak height of calcite which is an indication of the role of lime (CaO) in the formation of calcite ($CaCO_3$). The mica mineral phase also exhibited heterogeneous distribution in the drilled weathered cores which could be attributable to continuous weathering process.

1 year old core ash samples								
	An	**En**	**Ca**	**H**	**L**	**M**	**Mi**	**Q**
Mean	12776.3	13262.8	13614	13474.9	13128.2	13969	13310.4	33003.8
Stdev.	8198.9	8153.39	7813	7797.4	8057.18	7966.25	7759.5	12837.9
RSD %	64.17	61.48	57.39	57.87	61.37	57.03	58.30	38.90
8 year old ash core samples								
	An	**En**	**Ca**	**H**	**L**	**M**	**Mi**	**Q**
Mean	200.00	9261.54	1815.38	4453.85	10923.08	11692.31	3276.92	8600.00
Stdev.	0.00	83.56	170.28	381.53	2646.67	264.46	42.13	161.72
RSD %	0.00	0.90	9.38	8.57	24.23	2.26	1.29	1.88
20 year old ash core samples								
	An	**En**	**Ca**	**H**	**L**	**M**	**Mi**	**Q**
Mean	14955.4	10933.9	9302.0	10754.1	10291.0	10630.0	10513.0	37438.0
Stdev.	4862.3	5729.2	6515.9	5985.0	6284.1	6487.6	5980.7	9230.3
RSD %	32.5	52.4	70.0	55.7	61.1	61.0	56.9	24.7

[An=Anorthite, En=Enstatite, Q=Quartz, Mi=Mica, M=Mullite, Ca=Calcite, H=Hematite, L=Lime].

Table 1. Summary of the statistical analysis of the peak heights of various mineral phases in Tutuka fly ashes (1 year, 8 year and 20-year-old dry disposed cores)

Mullite showed variations (57-65 %) in the peak heights which might be due to the conversion of clays that contain < 60 % of Al_2O_3. The mullite peak heights depend on the amount of SiO_2 and Al_2O_3 in the mineral phase (Figure 4 and Table 1). Anorthite is a rare compositional variety of plagioclase feldspar (calcium rich end-member of plagioclase). Anorthite has been found in other fly ashes obtained from coals in which Ca is present in inherent minerals together with other minerals with which calcium reacts.

Anorthite showed variations (57-65 %) in peak height which could be due to chemical interactions of CaO, SiO_2 and Al_2O_3 in the mineral phase of coal fly ash samples. Enstatite is a magnesium silicate mineral. Enstatite shows variations (57-65 %) in peak heights due to prevailing chemical interactions of SiO_2 and MgO in the mineral phase of coal fly ash samples. Hematite (Fe_2O_3) is a heat transformation product of pyrite in feed coal and accordingly hematite was revealed by XRD in the ash core samples. Previous studies had shown that pyrite (FeS_2) was present in the feed coal as a fine-grained mineral [35]. Hematite (Fe_2O_3) phase showed variations (≈ 57 - 87 %) in peak heights distribution among the fly ash samples. This trend is an indication of the instability of the Fe containing mineral phases in the ash core samples of 1-year-old ash at the dry disposed fly ash dump site. The relative standard deviation (RSD) in the peak heights of the 8-year-old ash (Figure 5 and Table 1) showed low variations which could be classified into 3 groups:

< 3 % Anorthite, Enstatite, Quartz, Mica, Mulite,

< 10 % Calcite and Hematite

< 25 % Lime

The relative standard deviation (RSD) of anorthite, enstatite, quartz, mica and mullite (being < 3 %) indicates homogeneity among these coal fly ash mineral phases in this core. There was however more variation (< 25 %) in the mean peak heights of lime (CaO) in the 8-year-old ash samples. The in-homogeneous distribution of calcite and hematite mineral

phase (< 10 %) could be attributed to continuous differential weathering occasioned by chemical interaction of fly ash with atmosphere, ingressed carbon dioxide and percolating rain water.

The relative standard deviation (RSD) in the peak heights of the 20-year-old ash (Figure 6 and Table 1) showed moderate variations which could be classified into 3 groups:

< 35 % Anorthite

< 60 % Enstatite, Mica and Hematite

≤ 70 % Lime, Mullite and Calcite

There is obvious similarity in the variation of mineral peak height of 20 year and 1-year-old drilled cores (Figures 4 & 6) which is attributed to in-homogeneity due to textural differences in 1 year and 20-year-old drilled ash cores [34]. Less variation in the mineral phase peak heights is observed with the age of the ashes due to dissolution/precipitation of secondary phases (stability of mineral phases) with time. The decrease or increase in the mean peak height of some minerals in the 3 drilled ash cores suggest variation in the steady state conditions at the interface of mineral particles due to reduction in the ash pore water pH [34]. The RSD in the mineral peak heights showed correlation with already significant change in chemistry of the 3 drilled ash core samples. This showed that significant flushing/leaching of major components of fly ash had taken place within 1 year of ash dumping due to continuous irrigation with high saline effluents [34].

Bulk chemical composition as determined by XRF analysis of all the coal fly ash samples also revealed major presence of MgO in fly ash which could result in the formation of enstatite ($Mg_2Si_2O_6$) upon concomitant depletion of quartz. Mullite and quartz were the species identified, quartz being the only original unaltered coal mineral phase present [36]. Mullite and hematite are products of the thermal transformation of some minerals present in the coal during combustion. Mullite ($3Al_2O_32SiO_2$) is a product of aluminosilicate transformation. It has been reported that mullite in fly ash is formed through the decomposition of kaolinite, $Al_2Si_2O_5$ $(OH)_4$ [31, 35], which is entrapped in the parent coal. For UK fly ashes mullite is reported to form preferentially from kaolinite, whereas illite contributes towards the glass phase [35]. Calcite ($CaCO_3$) was found in all coal fly ash core samples. Calcite precipitation in weathered fly ash is as a result of chemical interactions of calcium oxide (lime) rich fly ash with ingressed CO_2 [32] during weathering. The high concentration of calcium oxide as evidenced by XRF analysis [34] of the core samples suggests possible secondary formation of anorthite ($CaAl_2Si_2O_8$), calcite, and lime in the fly ash dump [28]. Anorthite is a calcium mineral not present in coals. The formation of anorthite requires the mixing of separate calcium and aluminosilicate mineral domains. Thus, as calcium aluminosilicates are not found in fly ashes, their presence in coal-fired boiler deposits has been used to probe the mechanism of deposit formation. Studies of a range of coal fired boiler deposits, having different temperature histories, together with complementary investigations on mineral mixtures and coal ashes, have demonstrated that

anorthite is formed via solid-state reactions and not by recrystallization from a homogeneous melt [38].

3.3. FTIR spectral analysis of the coal sample

FTIR was used to identify the mineral matter components removed and to monitor any changes in the functional groups resulting due to microbial treatment in the raw and bioleached coals. Figure 2 shows the FTIR spectra obtained for raw and bioleached coals. All peaks between 3600 cm^{-I} to 413 cm^{-1} were enlarged separately.

The high mineral content of the coals necessitated the analysis of the mineral matter more closely. Distinct peaks at the regions of 1000, 529 and 413 cm^{-1} are ascribed to kaolinite [39, 40]. In kaolinite (1:1 layer silicate), one of the silicate anions is replaced by a sheet of hydroxyl groups, and the layer units are linked by hydrogen bonds between the hydroxyl surface of the layer and the oxygen surface of the next layer. The high frequency OH^- vibrations occur at the region of 3600 cm^{-1}. In dioctahedral silicates, the degree of substitution of aluminium (A1) for silicon (Si) is lower than in trioctahedral silicates [41]. A perpendicular Si-O vibration causes absorption at 413 to 529 cm^{-1}. The Si-O-Si stretching vibrations give two bands at 1594 and 2174 cm^{-1} Si-O bending vibrations contribute to the strong absorption at 413 and 529 crn^{-1}.

The presence of quartz in the coal sample possibly gives rise to the IR spectrum with absorption frequency at 746 and 684 cm^{-1} [42, 43, 44]. The potassium selenium chlorides also absorb at 1625 and 1450 cm^{-1}. The small shoulder at 1450 cm^{-1} could be attributed to potassium selenium chlorides. The spectra indicated that the coal sample used in the present study had little iron sulphide. The iron sulphide (pyrite) is generally the most important of the iron-bearing minerals in coals (basic absorption frequency 413 crn^{-1}). Previous study established that the presence of quartz in the 2-week-old ash gives rise to IR spectrum with absorption frequency at 433-427, 770-764, and 991-996 cm^{-1}. Although, the presence of mullite is responsible for the series of bands around 540-532 and 1,413-1,000 cm^{-1} [45].

3.4. Microscopic study of coal and coal ash

SEM can provide size and morphology information of particles at submicron scale [46]. The size and morphological characteristics of coal and coal ash particles examined by SEM are exemplified in Fig. 7. SEM observations show that the coal and coal ash particles The coal ash (Fig. 7c, d) consists mostly of spherical shaped and aggregate that contains varying sizes and amount of particles. Conversely, the coal sample consisted of irregular shaped pyrite crystal coated with kaolinite (Fig 7a, b). TEM is the most powerful and appropriate technique for investigating the characteristics of nanoscale particles [46]. The morphology of coal and coal ash were identified using TEM. Transmission electron microscopy (TEM) is the most powerful and appropriate technique for investigating the characteristics of nanoscale particles [46]. The morphology of coal and coal ash were identified using TEM. The TEM images show that the coal and coal ash are made up of

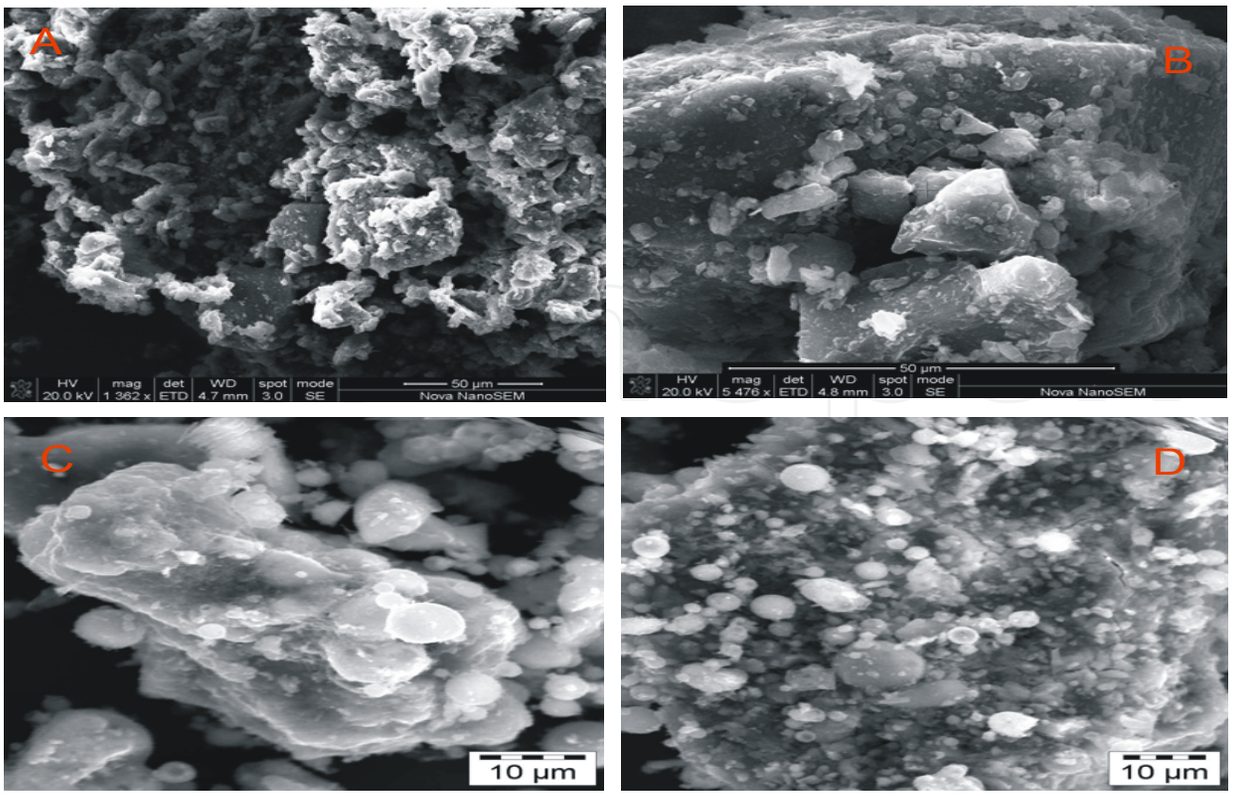

Figure 7. Scanning electron microscopy (SEM) of coal (a, b) and coal ash (c, d). Change the color of the letters so they are visible against the background of the photos

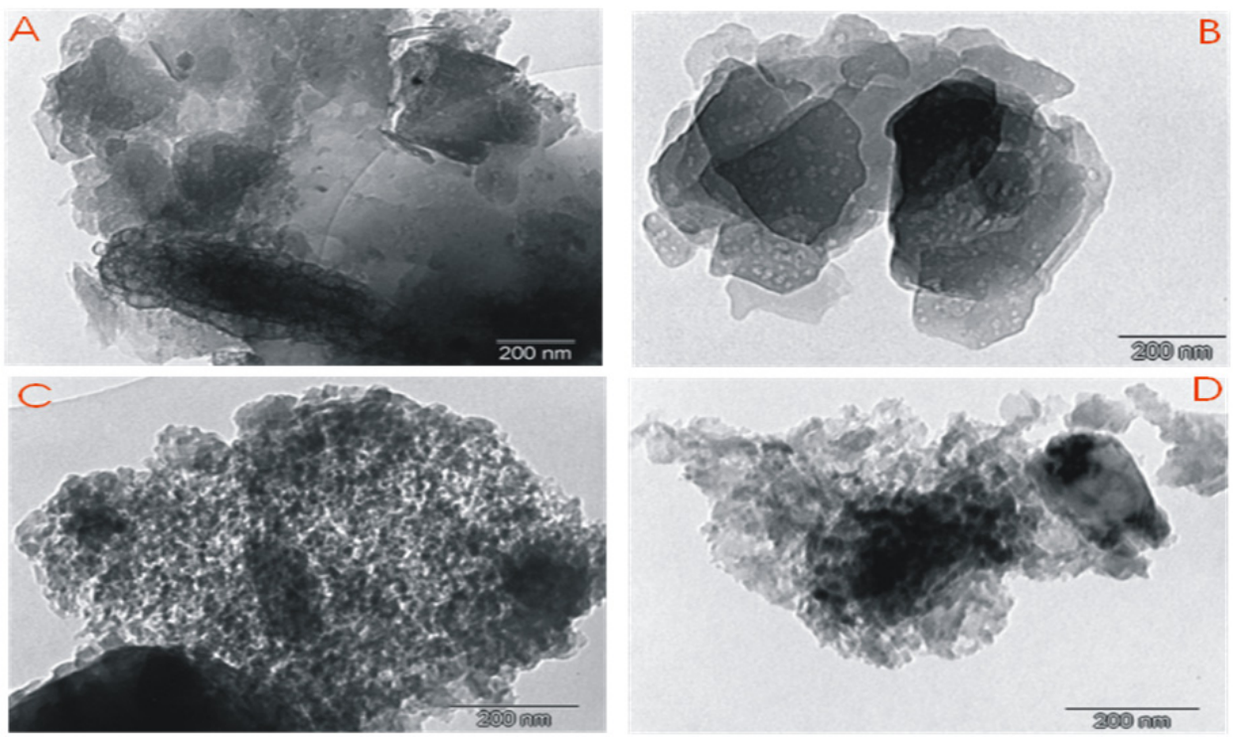

Figure 8. Transmission electron microscopy (TEM) of coal (a, b) and coal ash (c, d)

particles greater than 200μm. TEM images of coal ash sample showed nearly spherical shaped haematite structure (Fig. 8d), and cluster texture agglomeration of ultrafine particles (Fig. 8c). On the other hand, the TEM images shows that coal sample consist irregular shaped Fe-rich particles (i.e. pyrite) encrusted with Al, Si-rich particles (i.e. kaolinite) (Fig. 8 a, b). The metallifeorus particles such as Fe-rich particles, Al-rich particles and Si-rich particles are not uniformly distributed in the heterogeneous microstructure of coal ash [47, 48].

3.5. Geochemistry

Table 2 reports the chemical composition of coal and ash samples. The elements found in coals are commonly classified as major (> 1 wt. %), minor (1-0.1 wt. %) or trace (< 0.1 wt. %) elements. These elements may occur in both organic and inorganic constituents of coal and each element has dominant associations and affinities with different phases in coal [49]. The most abundant major components in both coal and ash samples are Si followed by Al, Fe and Ca. The least abundant components in the pulverised coal and fresh ash are Ti, Mg, Na, K, P, Cr and Mn. The bulk chemical composition and classification systems of coal fly ash always include data for LOI. The LOI and volatile (H_2O) components are relatively enriched in the pulverised coal sample. This combustion process thermally converts kaolinite to mullite as indicated in the Figures 1 & 2. This type of fly ash is principally composed of small (10 mm or less) glassy aluminosilicate spheres. The latter are formed by the rapid cooling of the molten mineral matter in the pulverized coal used in the power station boilers [50]. The ratio of Si/Al in the coal ash is ≥ 2 and thus can also be classified as silico-aluminate fly ash [51].

3.5.1. Major elements

Usually elements in coal occur either associated with the inorganic constituents (minerals) or with organic constituents [52]. The enrichment factor (EF) of the inorganic elements was calculated based on the method previously proposed by [53] (Table 2). Major elements such as Fe, Ca, Mg, Mn and Ti were as expected in coal samples but significantly enriched in the coal ash. Although, P, Na and K are slightly enriched in the coal ash samples used in this study. Enriched values in the ash were observed for environmentally significance trace elements.

3.5.2. Trace elements

The distribution of trace elements in coals used for electrical generation is of increasing importance in the assessment of environmental impacts from coal-fired power plants [54]. Trace elements such as U, Cr, Th, V, Ni, Cu, Zn, Rb, Sr, Mo and Sn are slightly enriched in the coal ash (Table 2).

The slight enrichment of these trace elements in the coal ash is attributed to the combustion process. Simultaneously, trace elements (such as Hf, Ta, Pb, Cr, Zr and Nb) showed

significant enrichment in the coal ash. On the contrary, W, As, Cs and Ba are considerably enriched in the coal samples used in the present study. In summary, most of the determined trace elements were comparatively enriched in the coal ash when compared with the parent material (coal). Therefore, the trace elements relative enrichment in coal ash is attributed to the combustion process in the Tutuka power station.

Concentration (ppm)									
Element	LLD	Coal	Coal ash	EF	Element	LLD	Coal	Coal ash	EF
Si		79200.0	238700.0	0.94	As		231.08	47.67	0.064
Al		60400.0	126400.0	0.65	V	0.06	54.77	117.41	0.67
Fe		2600.0	37000.0	4.43	Cr	1.26	53.77	187.64	1.09
Ca		1300.0	41700.0	9.98	Co	0.02	24.25	17.53	0.22
Mg		600.0	5900.0	3.06	Ni	0.22	18.94	57.92	0.95
Mn		100.0	400.0	1.24	Cu	0.68	39.96	46.30	0.36
K		5100.0	6700.0	0.41	Zn	0.31	38.80	53.99	0.43
Na		500.0	600.0	1.06E-05	Rb	0.04	30.28	37.21	0.38
P		1200.00	2000.0	0.52	Sr	0.00	614.01	1270.70	0.644
Ti		4200.00	13500.0	1.00	Zr	0.01	99.09	392.21	1.23
U	0.002	3.82	10.25	0.84	Nb	0.01	10.35	35.45	1.07
Hf	0.01	2.84	10.77	1.18	Mo	0.00	3.24	6.31	0.12
Ta	0.004	0.82	2.65	1.01	Sn	0.07	4.07	8.95	0.68
W	0.00	119.17	6.99	0.02	Cs	0.01	6.16	5.92	0.30
Th	0.003	14.40	36.39	0.79	Ba	0.06	1200.18	1062.15	0.28
Pb	0.02	8.49	38.50	1.41					

* EF = [(X) / (Ti)$_{Ash}$ / (X) / (Ti)$_{Coal}$], where X means element (Ogugbuaja and James, 1995)

Table 2. Major and trace elements in the coal sample and coal ash from Tutuka Power Station (*n = 3*) (*LLD = Low level detection*)

3.5.3. Rare Earth Elements (REE)

Rare earth elements (REEs) contents in the coal used in the present study are summarized in Table 3. It shows that the bulk of REEs are found in high levels in coal ash when compared with the typical concentration in coal. Rare earth elements (REEs) such as La, Ce, Pr, Nd, Sm, Eu and Gd are slightly enriched in the coal ash. On the contrary, Lu, Y, Dy, Tb, Yb, Tm, Er and Ho are considerably enriched in the coal ash used in the present study. Enrichment of REEs in the coal ash disagreed with the previously held views [55, 56]. Consequently, the obvious enrichment of REEs in the coal ash used in the present study is attributed to the combustion conditions. Rare earth elements in coal appear to consist of a primary fraction which is associated with syngenetic mineral matter [57]. Another portion of the REE can be externally derived or mobilized when primary mineral matter is destroyed or modified.

3.6. Genetic features relations of coal and coal ash based on chemical composition

Minerals in coal are both detrital and authigenic in nature and their distribution in the inorganic matter are variable. Authigenic minerals in coal are mainly sulfides, carbonates and sulfates of Fe, Mg and Ca [58]. The chemical composition in this detrital authigenic index (DAI) also symbolizes the different index mineral (IM) in coal. For example, the

oxides of Si, Al, K^+, Na^+, and Ti represent minerals and phases such as quartz, feldspars, clay and mica minerals (excluding some kaolinite and illite), volcanic glass, Al oxyhydroxide, and rutile-anatase-brookite, which commonly have dominant detrital genesis in coal. On the other hand, the oxides of Fe, Ca, Mg, S, P, and Mn represent minerals such as Fe-Mn sulphides; Ca-Fe-Mg sulphates, Ca-Mg-Fe-Mn carbonates and Ca-Fe phosphates, which commonly have dominant origin in coal [59]. Based on the ratio of detrital and authigenic minerals (DAI) some genetic information for the formation of fly ash could be deduced [51].

Concentration (ppm)				
Element	LLD	Coal	Coal ash	EF
La	0.002	39.90	91.36	0.71
Ce	0.004	91.61	182.42	0.62
Pr	0.002	9.46	19.72	0.65
Nd	0.016	30.84	71.76	0.72
Sm	0.009	5.30	14.38	0.84
Ho	0.003	0.67	2.35	1.09
Er	0.004	1.89	6.65	1.09
Tm	0.002	0.27	0.95	1.08
Yb	0.000	1.81	6.5	1.11
Eu	0.004	0.89	2.68	0.94
Gd	0.012	4.15	12.62	0.95
Tb	0.002	0.57	1.91	1.04
Dy	0.007	3.31	11.91	1.12
Y	0.01	17.50	64.87	1.15
Sc	0.12	9.66	26.50	0.85
Lu	0.002	0.25	0.93	1.15

* EF = [(X) / (Ti) $_{Ash}$ / (X) / (Ti) $_{Coal}$], where X means element (Ogugbuaja and James, 1995)

Table 3. Rare Earth Elements (REE) in the coal sample and coal ash from Tutuka Power Station (*n =3*) (*LLD = Low level detection*)

The main trend (Table 4) indicates that the coal used in the present study is a higher-ash coals which is enriched in elements associated with probable detrital minerals. Detrital minerals such as quartz, kaolinite, illite, acid plagioclases, muscovite, rutile, apatite and Fe and A1 oxyhydroxides are commonly stable minerals during coalification. Their proportions in coal may remain almost unchanged, while their total amount depends predominantly on the supply of clastic material into the peat swamp [23].

From Table 4, the proportion of detrital minerals is higher in coal sample used in the present study. It has been pointed out that the proportion of detrital minerals in coal increases [60]. The ratio of SiO_2/Al_2O_3 in the coal ash is ≥ 2 and thus can also be classified as silico-aluminate fly ash [51]. The bulk chemical composition and classification systems of coal fly ash always include data for LOI.

Major elements (%)										
Sample Name	SiO_2	Al_2O_3	Fe_2O_3	CaO	MgO	MnO	SiO_2/Al_2O_3	K_2O/Na_2O	$(MgO+CaO)/(K_2O+Na_2O)$	DAI
SAC	16.94	11.41	0.37	0.18	0.12	0.01	1.48	4.46	0.40	24.53
FA	51.05	23.88	5.29	5.84	1.26	0.05	2.14	5.37	7.39	5.97
Sample Name	Cr_2O_3	TiO_2	K_2O	Na_2O	P_2O_5	LOI	SO_3	Sum	CaO/MgO	
SAC	0.01	0.44	0.62	0.14	0.28	67.92	0.25	98.67	1.44	
FA	0.03	1.40	0.81	0.15	0.45	8.51	0.05	98.76	4.63	

DAI: ($(SiO_2+Al_2O_3+K_2O+Na_2O+TiO_2)$ / $(Fe_2O_3+CaO+MgO+SO_3+P_2O_5+MnO)$).

Table 4. Genetic features of coal and coal ash based on chemical composition

[61] classified fly ash based on the intersection of the sum of their major oxides: sialic: $SiO_2+Al_2O_3+TiO_2$; calcic: $CaO+MgO+NaO_2+K_2O$; and ferric: $Fe_2O_3+MnO+P_2O_5+SO_3$ in a ternary diagram. Based on the chemical composition of coal ash, about seven intermediate fly ash subgroups exists, such as sialic, ferrosialic, calsialic, ferrocalsialic, ferric, calcic and ferrocalcic [51] fly ash. The 1-year-old ash core samples were both sialic and ferrocalsialic in chemical composition (i.e. essentially Fe, Ca, Al and Si). Although, the 2 week and 20-year-old dry disposed ash core samples were sialic in chemical composition (i.e. essentially dominated by Al and Si) (Fig. 8). These trends show that in the 1-year-old drilled cores, there is already a significant change in chemistry of ash core due to rapid weathering or due to irrigation with high saline effluents. The coal fly ash transforms into a more clay-like material due to long-term mineralogical changes occasioned by the weathering process.

3.7. Proximate analysis and coal quality

The result obtained from proximate and ultimate analyses of pulverised coal sample is given in Table 5. The moisture and ash contents on dry and wet basis of pulverised coal sample (0.8 %; 94.43 %; 93.67 %) respectively. These values are higher than the Polish coals (0.58 %; 4.79 %) but the American coal (1.07 %; 5.77 %) was significantly higher in the moisture content. Some Nigerian coal deposits such as Lafia-Obi (2.91 %; 8.7 %) and Chikila coals (5.82 %; 14.9 %) also have considerably higher moisture content [62]. The relatively low moisture content in the pulverised coal sample represents a significant improvement in coal's quality because moisture affects the calorific value and the concentration of other constituents [63]. Nevertheless, the ash content of American coal, Lafia-Obi and Chikila coals are relatively lower than the ash content on dry basis of the pulverised coal used in this study. Similarly the low ash content is an improvement on the coking quality, low ash content is an essential requirement for coke making coals [63].

Therefore the pulverised coal used in this study may be expected not to have good coking qualities. An ash content of less than 10 % is recommended for a good coking coal (Bustin et al., 1985). Industrial experience indicates that a 1 wt. % increase of ash in the coke reduces metal production by 2 or 3 wt. % [65].

The volatile matter on dry and wet basis of pulverised coal sample is (5.6; 6.3) respectively (Table 5). The volatile matter of the pulverised coal sample used in this study is considerable lower than the American coal (31.36 %), Polish coal (32.61 %), Lafia-Obi (29.37 %) and Chikila (44.27 %) [66, 62]. Volatile matter, apart from its use in coal ranking, is one of the most important parameters used in determining their suitable applications [67]. Volatile matter does not form part of the coal; it is usually evolved as tar during carbonization. High-volatile bituminous coal due to its high volatile matter content generates high pressure during carbonization which is detrimental to the coke oven walls ([68, 69]. The above-mentioned data indicated that the coal used in the present study can be classified as medium volatile bituminous coal according to ASTM specification [70].

The elemental composition and elemental ratios of the coal sample used in this study are listed in Table 5. The obtained values for C, N and H contents are within the range observed for various types of coal [66, 62]. The C/N ratios of coal sample used in this study are higher than those reported for two south Brazilian coals [71]. On the other hand, similar values of H/C ratios observed in the present study have been obtained from two south Brazilian coals [71]. The fixed carbon of coal sample used in this study is 45.75 %. This is relatively higher than fixed carbons obtained from Chikila (40.83 %) coal. On the contrary, it is considerably lower than the fixed carbons in the Lafia-Obi (61.93 %), American (62.87 %) and Polish (62.60 %) coals [66, 62]. The carbon content of a coal is essential in coke making because it is the mass that forms the actual coke [72]. Therefore based on the fixed carbon the coal used in this study may be expected not to have good coking qualities.

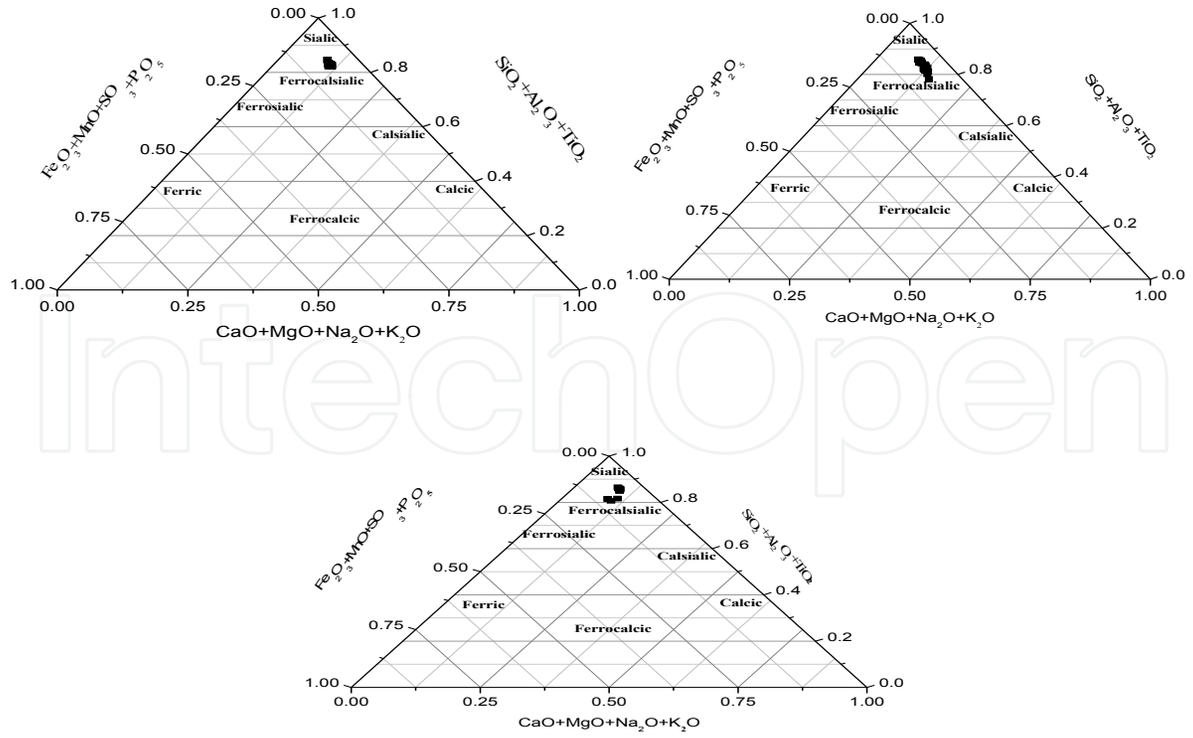

Figure 9. Ternary oxide plots for classification of the ash dumps: (a) 2-week-old (T 87) not irrigated dry ash dump (b) 1-year-old (AMB 83) irrigated and quenched with high salient effluents (n = 2) (c) 20-year-old irrigated and quenched with fresh water.

Proximate analysis of coal sample						
Sample	% Moisture	% Ash (dry basis)	% Ash (wet basis)	Volatile matter (dry)	Volatile matter (wet)	
SAC	0.8	94.43	93.67	5.6	6.3	
Ultimate analysis of coal sample						
Sample	N %	C %	H %	C/N	H/C	OM %
SAC	1.16	45.75	3.50	39.55	0.08	77.78

Note: OM % = C %*1.7.

Table 5. Proximate and ultimate analyses of South African coal sample *(n = 3)*

The organic matter content calculated (OM %) was calculated from the carbon content by multiplying with a value of 1.7 (Table 3). The derived organic matter content of the coal sample used in the present study is comparatively higher than Lafia-Obi coal (Jauro et al., 2008; Nasirudeen and Jauro, 2011).

4. Conclusions and summary

The XRD spectra showed that the coal sample mainly composed of siliceous mineral (such as quartz and kaolinite) and the non-siliceous mineral (such as potassium selenium chloride) and little quantities of pyrite. The results of the XRD analysis of samples of the drilled weathered dry disposed fly ash aged 2 week, 1 year and 20-year-old showed quartz and mullite as main crystalline mineral phases. Other minor mineral phases identified are; hematite, calcite, lime, anorthite, mica and enstatite.

The IR spectrum revealed the presence of quartz, kaolinite, potassium selenium chloride and pyrite in coal sample. SEM image of coal ash reveals spherical shaped and aggregate that contains varying sizes and quantity of particles. Conversely, the coal sample consists of irregular shaped pyrite crystal coated with kaolinite. TEM images of coal ash sample show nearly spherical shaped haematite structure and cluster texture agglomeration of ultrafine particles. Conversely, the TEM images of coal sample show irregular shaped Fe-rich particles (i.e. pyrite) encrusted with Al, Si-rich particles (i.e. kaolinite).

The main trend in the major oxides indicates that the coal used in the present study is a higher-ash coals which is enriched in elements associated with probable detrital minerals. The 1-year-old ash core samples were both sialic and ferrocalsialic in chemical composition (i.e. essentially Fe, Ca, Al and Si). Although, the 2 week and 20-year-old dry disposed ash core samples were sialic in chemical composition (i.e. essentially dominated by Al and Si).

Major elements such as Fe, Ca, Mg, Mn and Ti were as expected in coal samples but significantly enriched in the coal ash. Although, P, Na and K are slightly enriched in the coal ash samples used in this study.

Trace elements such as U, Cr, Th, V, Ni, Cu, Zn, Rb, Sr, Mo and Sn are slightly enriched in the coal ash. This slight enrichment of these trace elements in the coal ash is attributed to the combustion process. Nevertheless, trace elements (such as Hf, Ta, Pb, Cr, Zr and Nb)

showed significant enrichment in the coal ash. On the contrary, W, As, Cs and Ba are considerably enriched in the coal samples used in the present study.

Rare earth elements (REEs) such as La, Ce, Pr, Nd, Sm, Eu and Gd are slightly enriched in the coal ash. On the contrary, Lu, Y, Dy, Tb, Yb, Tm, Er and Ho are considerably enriched in the coal ash used in the present study.

The proximate analysis revealed that the moisture content, ash content and volatile organic matter of pulverised coal used in this study is relatively low in values compare to the American coal, Polish coal, Lafia-Obi and Chikila coals. The ultimate analysis showed that the fixed carbon of coal sample used in this study is relatively higher than fixed carbons obtained from Chikila coal. On the contrary, it is comparatively lower than the fixed carbons in the Lafia-Obi, American and Polish coals

In conclusion, factors such as the nature of combustion process, type of coal and chemical interaction of fly ash with the ingressed CO_2 and percolating rain water would ultimately determine the mineralogy and chemical composition of coal combustion products.

Author details

S. A. Akinyemi, A. Akinlua
Fossil Fuel and Environmental Geochemistry Group, Department of Earth Sciences; University of the Western Cape, Bellville, South Africa

L. F. Petrik
Environmental and Nano Sciences Group, Department of Chemistry; University of the Western Cape, Bellville, South Africa

W. M. Gitari
Environmental Remediation and Water Pollution Chemistry Group, Department of Ecology and Resources Management, School of Environmental Studies, University of Venda. X5050, Thohoyandou, South Africa

5. References

[1] Jeffrey, L. S. Characterization of the coal resources of South Africa. The Journal of the South African Institute of Mining and Metallurgy 2005; 95-102.
[2] DME (Department of Minerals and Energy), Digest of South African Energy Statistics. Department of Minerals and Energy, Pretoria. 2005.
[3] Daniel, M. African coat supply prospects, lEA Coal Research, London, 1991.
[4] Snyman, C. P. and W. J. Botha, W. J. Coal in South Africa. Journal of African Earth Sciences, 1993; 16 171-180.
[5] Renton, J. J. Mineral matters in coal, In: Meyers, R. A. (Ed.). *Coal Structure*. New York Academy Press. 1982.

[6] Kolker, A.; Finkelman, R. B.; Palmer, C. A.; & Belkin, H. E. Arsenic, mercury and other trace metals in coal: Environmental and health implications (Abstract, International Ash Utilization Symposium, Lexington, KY); 2001.

[7] Burgers, C. L. Synthesis and characterization of sesquioxidic precipitates formed by the reaction of acid mine drainage with fly ash leachate. Unpublished M.Sc. Thesis, University of Stellenbosch, South Africa; 2002.

[8] Bezuidenhout, N. Chemical and mineralogical changes associated with leachate production at Kriel power station ash dam. Unpublished M.Sc. Thesis, University of Cape Town, Cape Town, South Africa; 1995.

[9] Petrik, L. F., White, R. A., Klink, M. J., Somerset, S. V., Burgers, L. C., and Fey, V. M.. Utilization of South African fly ash to treat acid coal mine drainage, and production of high quality zeolites from the residual solids. International Ash Utilization Symposium, Lexington, Kentucky; October 20–22. 2003.

[10] Eskom abridged annual report. (2009). Available at www.eskom.co.za, Accessed on 23rd May, 2010.

[11] Basham, K., Clark, M., France, T., and Harrison, P. What is fly ash? Fly ash is a by-product from burning pulverized coal in electric power generating plants. Concrete Construction Magazine; November 15. 2007.

[12] American Society for Testing and Materials. Annual Book of ASTM Standards, Section 5: Petroleum Products, Lubricants and Fossil Fuels. 5.05: Gaseous Fuels; Coal and Coke; 1992.\

[13] Vassilev, S. V. Trace elements in solid waste products from coal burning at some Bulgarian thermoelectric power stations. Fuel 1994a; 73 367-374.

[14] Querol, X., Fernández-Turiel, J. L., Lopez-Soler, A. Trace elements in coal and their behaviour during combustion in a large power station. Fuel 1995; 74 331.

[15] Vassileva, G. G., Vassilev, S. V. Behaviour of inorganic matter during heating of Bulgarian coals 1. Lignites. Fuel Processing Technology 2005; 86 1297-1333.

[16] Vassileva, C. G., Vassilev, S. V. Behaviour of inorganic matter during heating of Bulgarian coals 2. Sub bituminous and bituminous coals Fuel Processing Technology 2006; 87 1095–1116.

[17] Silva, L. F.O., Ward, C. R., Hower, J. C., Izquierdo, M., Waanders, F., Oliviera, M. L. S., Li, Z., Hatch, R. S., Querol, X. Mineralogy and Leaching Characteristics of Coal Ash a Major Brazilian Power Plant. Coal Combustion and Gasification Products 2010; 2 51-65.

[18] Ward, C. R., Spears, D. A., Booth, C. A., Staton, I. Mineral matter and trace elements in coals of the Gunnedah Basin, New South Wales, Australia. Int J Coal Geol. 1999; 40 (4) 281–308.

[19] Querol X, Alastuey A, Lopez-Soler A, Plana F, Zeng RS, Zhao J, et al. Geological controls on the quality of coals from the West Shandong mining district, Eastern China. Int J Coal Geol. 1999; 42 (1) 63–88.

[20] Liu, G., Vassilev, S. V., Gao, L., Zheng, L., Peng, Z. Mineral and chemical composition and some trace element contents in coals and coal ashes from Huaibei coal field, China. Energy Conversion and Management 2005; 46 2001–2009.

[21] Gluskoter, H. J. Mineral Matter and Trace Elements in Coal. In Trace Elements in Fuel; Babu, S.; Advances in Chemistry; American Chemical Society: Washington, DC. 1975.

[22] Liu, G. J., Yang, P. Y., Chou, C. L., Peng, Z. C. Petrographical and geochemical contrasts and environmentally significant trace elements in marine-influenced coal seams, Yanzhou Mining Area, China. J Asian Earth Sci. 2004; 24 (3) 491–506.

[23] Vassilev, S. V., Kitano, K., and Vassileva, C. G. Relations between ash yield and chemical and mineral composition of coals. Fuel 1997b; 76, (1) 3-8.

[24] McCarthy, G. J., Swanson, K. D., Keller, L. P., and Blatter, W. C.. Mineralogy of Western fly ash Cement and Concrete Research 1984; 14 471-478.

[25] Filippidis A., Georgakopoulos**,** A. Mineralogical and chemical investigation of fly ash from the Main and Northern lignite fields in Ptolemais, Greece. Fuel 1992; 71 373-376.

[26] Vassilev, S. V., Vassileva, C. G. Mineralogy of combustion wastes from coal-fired power stations. Fuel Process Technol. 1996a; 47 261–280.

[27] Sakorafa, V., Burragato, F., Michailidis, K. Mineralogy, geochemistry and physical properties of fly ash from the Megalopolis lignite fields, Peloponnese, Southern Greece. Fuel 1996; 75 419–23.

[28] Bayat, O. Characterization of Turkish fly ashes. Fuel 1998; 77 1059-1066.

[29] Koukouzas, N. K., Zeng, R., Perdikatsis, V., Xu, W., Emmanuel K. Kakaras, E. K. Mineralogy and geochemistry of Greek and Chinese coal fly ash. Fuel 2006; .85 2301–2309.

[30] Navarro, C. R., Agudo, E. R., Luque, A., Navarro, A. B. R., Huertas, M. O. "Thermal decomposition of calcite: Mechanisms of formation and textural evolution of CaO nanocrystals",American Mineralogist 2009; 94 578-593.

[31] White, S. C., and Case, E. D. Characterization of fly ash from coal-fired power plants. J. Mater. Sci. 1990; 25 5215–5219.

[32] Soong, Y., Fauth, D. L., Howard, B. H., Jones, J. R., Harrison, D. K., Goodman, A. L., Gray, M. L., and Frommell, E. A. CO_2 sequestration with brine solution and fly ashes. Energy Convers. Manage. 2006; 47 1676–1685.

[33] Stevenson, R. J., McCarthy, G. J. Mineralogy of Fixed-Bed Gasification Ash Derived from North Dakota Lignite. Mat. Res. Soc. Symp. Proc. 1985; Vol. 65.

[34] Akinyemi, S. A. Geochemical and mineralogical evaluation of toxic contaminants mobility in weathered coal fly ash: as a case study, Tutuka dump site, South Africa. Unpublished PhD thesis, University of the Western Cape, South Africa; 2011a.

[35] Spears, D. A. and Martinez-Tarazona, M. R. Geochemical and mineralogical characteristics of a power station feed-coal; Eggborough, England, Int. J. Coal Geol. 1993; 22 1-20.

[36] Bandopadhyay, A. K. "A study on the abundance of quartz in thermal coals of India and its relation to abrasion index: Development of predictive model for abrasion", International Journal of Coal Geology 2010; 84 63-69.

[37] Spears, D. A. Role of clay minerals in UK coal combustion. Applied Clay Science 2000; 16 87–95.

[38] Unsworth, J. F., Barratt, D. J., Park, D., Titchener, K. J. Ash formation during pulverized coal combustion. 2. The significance of crystalline anorthite in boiler deposits. Fuel 1988; 67 632- 642.

[39] Farmer, V. C. The infrared spectra of minerals. London: Mineralogical Society; 1987.

[40] Sharma, D.K. & Gihar, S. Chemical cleaning of low grade coals through alkali-acid leaching employing mild conditions under ambient pressure conditions. Fuel, 1991; 70 663-665.

[41] Sharrna, D. K and Wadhwa, G. Demineralization of coal by stepwise bioleaching: a comparative study of three Indian coals by Fourier Transform Infra-Red and X-ray diffraction techniques. World Journal of Microbiology & Biotechnology 1997; 13 29-36.

[42] Criado, M., Fernández-Jimènez, A., and Palomo, A. Alkali activation of fly ash: Effect of the SiO_2/Na_2O ratio. Part I: FTIR study. Microporous & Mesoporous Mater. 2007; 106 180–191.

[43] Fernandez-Carrasco, L., and Vazquez, E. Reactions of fly ash with calcium aluminate cement and calcium sulphate. Fuel 2009; 88 1533–1538.

[44] Mollah, M. Y. A., Promreuk, S., Schennach, R., Cocke, D. L., and Guler, R. Cristobalite formation from thermal treatment of Texas lignite fly ash. Fuel 1999; 78 1277–1282.

[45] Akinyemi, S. A., Akinlua, A., Gitari, W. M., and Petrik, L. F. Mineralogy and Mobility Patterns of Chemical Species in Weathered Coal Fly Ash Energy Sources, Part A 2011b; 33 768–784.

[46] Utsunomiya, S., Ewing, R. C. Application of high-angle annular dark field scanning transmission electron microscopy, scanning transmission electron microscopy energy-dispersive X-ray spectrometry, and energy-filtered transmission electron microscopy to the characterization of nanoparticles in the environment. Environmental Science & Technology 2003; 37 786–791.

[47] Silva L. F. O., Moreno, T., Querol, X. An introductory TEM study of Fe-nanominerals within coal fly ash. Science of the Total Environment 2009; 407 4972–4974.

[48] Akinyemi, S. A., Akinlua, A., W. M. Gitari, W. M., Nyale, S. M., Akinyeye, R. O., Petrik, L. F. An Investigative Study on the Chemical, Morphological and Mineralogical Alterations of Dry Disposed Fly Ash During Sequential Chemical Extraction. Energy Science and Technology 2012; 3 (1) 28-37.

[49] Vassilev, S. V., Vassileva, C. G. Geochemistry of coals, coal ashes and combustion wastes from coal-fired power stations. Fuel Processing Technology 1997a; 5 1 19-45.

[50] Foner. H. A., and Robl, 1 T. L. Coal Use and Fly Ash Disposal in Israel. Energeia 1997; 8, (5) 1-6.

[51] Vassilev S. V. and Vassileva, C. G. A new approach for the classification of coal fly ashes based on their origin, composition, properties and behaviour. Fuel 2007; 86 1490-1512.

[52] Zhang, J., Ren, D., Zheng, C., Zeng, R., Chou, C.-L., Liu, J. Trace element abundances of major minerals of Late Permian coal from southwestern Guizhou province, China. Int. J. Coal Geol. 2002; 53 55–64.

[53] Ogugbuaja, V. O., James, W. D. INAA multielemental analysis of Nigerian Bituminous Coal and Coal ash. Journal of Radioanalytical and Nuclear Chemistry, Articles 1995; 191 181-187.

[54] Karayigit, A.I., Gayer, R.A., Ortac, F.E., Goldsmith, S. Trace elements in the Lower Pliocene fossiliferous kangal lignites, Sivas, Turkey. Int. J. Coal Geol. 2001; .47 73–89.

[55] Swaine, D. J. Trace Elements in Coal. Butterworths, London. 1990; p. 278.

[56] Baioumy, H. M. Mineralogical and geochemical characterization of the Jurassic coal from Egypt. Journal of African Earth Sciences 2009; 54 75–84.

[57] Palmer, C. A., Lyons, P. C., Brown, Z.A., Mee, J. S. The use of trace element concentrations in vitrinite concentrates and companion whole coal (hvA bituminous) to determine organic and inorganic associations. GSA Spec. Pap. 1990; 248 55–62.

[58] Vassilev, S., Yossifova, M. and Vassileva, CInternational Journal of Coal Geology 1994b; 26 185.

[59] Vassilev S.V., Vassileva C. G. Occurrence, abundance and origin of minerals in coals and coal ashes. Fuel Proc. Technol. 1996b; 48 85-106.

[60] Finkelman, R. B. Scanning Microscopy 1988; 2 (1). 97.

[61] Roy, W. R., Griffin, R. A. A proposed classification system for coal fly ash in multidisciplinary research. Journal of Envir. Qual. 1982; 11 563-568.

[62] Nasirudeen, M. B. and Jauro, A. Quality of Some Nigerian Coals as Blending Stock in Metallurgical Coke Production. Journal of Minerals & Materials Characterization & Engineering 2011; 10, (1) 101-109.

[63] International Energy Agency (IEA)/Organization for Energy Co-operation and Development (OECD), Coal in the energy supply of India, Paris; 2002. p. 28.

[64] Bustin, R. M., Cameron, A. R., Greve, D. A. and Kalkreuth, W. D. Coal Petrology: Its Principles, methods and applications. Geological Association of Canada. Course Notes 1985; 3 230.

[65] Diez, M. A., Alvarez, R. and Barriocanal, C. "Coal for metallurgical coke production: Prediction of coke quality and future requirements for coke making." Int. J. Coal Geol. 2002; 50 289-412.

[66] Jauro, A., Chigozie , A. A. & Nasirudeen, M. B. Determination of selected metals in coal samples from Lafia-Obi and Chikila. Science World Journal 2008; 3 (2) 79-81.

[67] Peng Chen. "Petrographic Characteristics of Chinese coals and their applications in coal Utilization Processes." Fuel 2002; 81 11-12.

[68] Barriocanal, C., Patrick, J. W., and Walker, A. "The laboratory identification of dangerously coking coals." Fuel 1997; 77 881-884.

[69] Walker, R., Mastalerz, M., and Padgett, P. "Quality of selected coal seams from Indiana: Implications for carbonization." Int. J. of Coal Geol., 2001; 47 277-288.

[70] American Society for Testing and Materials. Annual Book of ASTM Standards, 5–6, p. 650. [71] Dick, D. P., Mangrich, A. S., Menezes, S. M. C. and Pereira, B. F. 2002. Chemical and Spectroscopical Characterization of Humic Acids from two South Brazilian Coals of Different Ranks J. Braz. Chem. Soc. 2002; 13 (2) 177-182.

[71] Price, J., Gransden, J., and Hampel, K. Microscopy, Chemistry and Rheology tools to determine Coal and Coke Characteristics. 1st McMaster's coke making course. McMaster's University Hamilton, Ontario, Canada; 1997.1-4 74.

IntechOpen